Atlantis Highlights in Engineering, volume 6

14th International Renewable Energy Storage Conference 2020 (IRES 2020)

Use of Pressurized Oxidation of Cu_2O as a Means of Improving the Performance of Redox Based Thermochemical Energy Storage Systems

Sike Wu
Priority Research Centre for Frontier Energy Technologies & Utilization
The University of Newcastle
Newcastle, Australia
sike.wu@uon.edu.au

Cheng Zhou
Priority Research Centre for Frontier Energy Technologies & Utilization
The University of Newcastle
Newcastle, Australia
cheng.zhou@newcastle.edu.au

Behdad Moghtaderi
Priority Research Centre for Frontier Energy Technologies & Utilization
The University of Newcastle
Newcastle, Australia
behdad.moghtaderi@newcastle.edu.au

***Abstract*— CuO/Cu_2O is a promising redox pair for thermochemical energy storage. This is primarily because of its suitable reaction temperature, high reaction enthalpy, high oxygen-carrying capacity, wide availability, and competitive cost. In this study, the influence of pressurized oxidation on a pure CuO/Cu_2O-based thermochemical energy storage system is examined experimentally. Specifically, thermogravimetric analyses (TGA) and scanning electron microscopy (SEM) are employed to assess the reaction characteristics and morphology changes of pure CuO/Cu_2O. According to the results, the oxidation of Cu_2O (the rate-limiting step) is found to be faster and more complete under a pressure of 5.0-15.0 bar compared to the near-ambient pressure under 1.2 bar. Meanwhile, the tests of 20 redox cycles reveal that the reactivity of Cu_2O can maintain 70-90%, but the agglomeration of particles is still present as a potential issue. The concept of pressurized oxidation is then applied to a utility-scale thermochemical energy storage plant in a case study. Based on the case study, the proposed storage plant can achieve a round-trip efficiency of about 41.0% and an energy storage density of nearly 500 kJ/kg under the oxidation pressure of 10.0 bar.**

Keywords*— *thermochemical energy storage, copper oxide, redox cycle, pressurized oxidation, thermogravimetric analysis

I. INTRODUCTION

Renewable energy has shown fast development in recent years. For instance, in 2018, the installed capacity of renewable energy, which occupied nearly 25% of the worldwide power generation, was increased by 450 TWh [1]. This remarkable development can be attributed to the significant advantages of renewable energy over fossil fuels regarding cleanness and sustainability [2]. Nevertheless, the fast-developing renewable energy also poses increasing challenges to the current power grid. Specifically, renewable energy, particularly solar and wind, are subject to weather, time, and location [3]. This intermittent nature, therefore, makes the power supply of renewable energy unstable. As a result, the stability and safety of the power grid with a high penetration of renewable energy are difficult to be maintained [4].

A promising solution to achieve a stable power supply of renewable energy is to employ energy storage technologies [5]. With energy storage, intermittent renewable energy can be stored in the other forms (e.g., mechanical, thermal, electrochemical, and etc.) that can be recovered in a later time when a stable power supply is needed [6]. Also, the excess renewable energy generated during the off-peak time can also be temporarily stored for later uses, which helps improve energy use efficiency. A wide variety of energy storage technologies emerged in the past years and some of which have been commercialized (e.g., pumped hydro storage, compressed air energy storage, and batteries) [7]. However, these commercialized energy storage technologies suffer from one or more significant disadvantages, such as low energy storage density, geographical constraints [8], high capital costs, poor scalability, and negative environmental impacts [9]. To overcome these disadvantages, various novel energy storage concepts have been developed recently. Among them, thermochemical energy storage (TCES) has attracted increasing research attention primarily because it shows no geographical limitations, excellent scalability, small environment concerns, and low expected costs [10].

TCES is usually realized by using a pair of reversible chemical reactions - an endothermal reaction and an exothermal reaction. Various TCES systems have been proposed and these systems are mainly based on metal oxides, hydrides, carbonates, hydroxides, ammonia, and organics [11]. It should be noted that the TCES system using metal oxides is attractive owing to its high operating temperatures, high reaction enthalpies, long storage periods, oxygen production, and utilization of air as the reactant and heat transfer medium. In the TCES systems based on metal oxides, the endothermal and exothermal reactions are represented by the reduction and oxidation, respectively. Wong et al. reviewed the metal oxides used in the TCES systems and concluded that Fe_2O_3/Fe_3O_4, BaO/BaO_2, Co_3O_4/CoO, Mn_2O_3/Mn_3O_4, and CuO/Cu_2O are more suitable than other material candidates in terms of reversibility, temperature range, cost, and reaction enthalpy [12].

Compared to other material candidates, CuO/Cu_2O presents a high reaction temperature of around 1000 °C, high reaction enthalpy of nearly 811 kJ/kg, excellent oxygen-carrying capacity, wide availability [13], and low cost. These features make CuO/Cu_2O considerably competitive in TCES applications. Fig. 1 illustrates the schematic diagram of a TCES system based on the redox pair of CuO/Cu_2O.

As can be seen from Fig. 1, the energy storage function of the CuO/Cu_2O-based TCES is realized by two steps, namely charging and discharging. In the charging step, CuO is reduced to Cu_2O by absorbing external heat via the endothermal reaction. The external heat can be sourced either directly from concentrated solar heat or indirectly from the heat produced by Joule heating using abandoned off-peak electricity. Meanwhile, oxygen is also produced in this step, which can be further used for various purposes and thus helps improve economic performance. In the discharging step, the produced Cu_2O in the charging step is then oxidized back to CuO by the oxygen in the incoming air. As a result, the stored heat is released to the air due to the exothermal oxidation. The heated air can then be used for generating power by employing efficient power cycles and the reproduced CuO is stored for the next charging-discharging cycle.

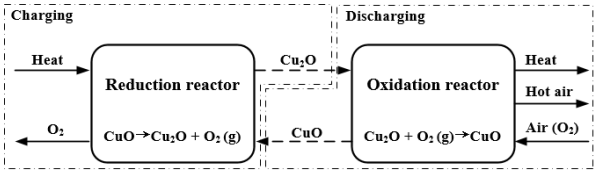

Fig. 1. Schematic diagram of a TCES system based on CuO/Cu_2O

Chadda et al. first studied the storage potential of CuO/Cu_2O in TCES in 1989 [14]. The research shows that the activation energy of reduction and oxidation were 313.0 kJ/mol and 76.5 kJ/mol, respectively. Wong et al. found that the oxidation temperature of Cu_2O was lower than its equilibrium reaction temperature, which makes the heating requirement of oxidation more accessible [12]. Meanwhile, they also mentioned that there was a high potential of sintering because the melting temperature of Cu_2O is considerably close to the reduction temperature of CuO. This finding was also observed in Deutsch et al.'s study in which sintering occurred in the CuO/Cu_2O sample tested in a packed bed [15]. To avoid the sintering risk, Alonso et al. employed a rotary kiln, which kept rotating the CuO/Cu_2O particles [16]. By using the rotary kiln, the sintering problem was relieved but only 40% of the raw material was found to be reduced in the air.

Regarding the utility-scale performance, Wu et al. proposed a phase change redox (PCR) system that further utilizes the melting/solidification process of CuO/Cu_2O [17]. The thermodynamic analysis showed that the PCR system could achieve a round-trip efficiency of nearly 51.1% and the experiment results successfully validated the key energy storage mechanism. Nevertheless, the oxidation step was designed to operate at 12.5 bar but the experiments were undertaken under atmospheric pressure. Meanwhile, Haseli et al. developed a similar utility-scale system for the TCES application of CuO/Cu_2O where the oxidation of Cu_2O took place at around 20 bar [18]. In a further study conducted by the same research group, Mahyar et al. confirmed that 2-5% of Cu_2O could be oxidized in the liquid state. However, the studied partial pressure of oxygen only varied between 0.2 bar and 0.8 bar [19]. Saman et al. examined the oxidation of Cu_2O at different oxygen partial pressures (i.e., 0.1, 0.2, 0.5, and 1.0 bar) using thermogravimetric analysis (TGA). The researchers concluded that the best conversion model was a two-dimensional Avrami-Erofeev model with an activation energy of 233 kJ/mol [20].

According to the literature review, the pressurized oxidation of Cu_2O is commonly found in the utility-scale concepts of CuO/Cu_2O-based TCES. This is primarily because, with the pressurized oxidation, the produced hot air under high pressure in the discharging step (see Fig. 1) can be directly used in an air Brayton cycle. This integration with the air Brayton cycle allows for a fast plant start-up and also makes the storage plant compact. Nevertheless, experimental studies of the pressurized oxidation of Cu_2O are rather limited in the literature. To have a better understanding of the pressurized oxidation of Cu_2O in the TCES applications thus becomes the main objective of the current study.

In this study, the pressurized oxidation of Cu_2O is initially studied via experiments. Specifically, TGA and scanning electron microscopy (SEM) are both applied to assess the reaction characteristics and morphology changes of CuO/Cu_2O in redox reactions. Besides the experiments, the concept of pressurized oxidation is also further investigated in a case study where a utility-scale TCES plant based on CuO/Cu_2O is developed. A thermodynamic analysis is carried out in this case study with a focus on the utility-scale storage performance of the developed plant, including but not limited to round-trip efficiency and energy storage density.

II. METHODS

Both experimental and modeling approaches are applied in the current study. Specifically, thermogravimetric analyses are conducted in the experiment and modeling work is implemented in the case study.

A. Experimental study

The raw material - CuO powder - with a purity of over 98% is obtained from Sigma Aldrich. The particle sizes of the CuO powder are below 10 μm. In each test, around 20 mg of CuO is weighed for the experiment. The gases flowing through the samples include N_2 (COREGAS, $N_2 \geq 99.999\%$) and air (COREGAS, $O_2 = 21.0 \pm 1.0\%$). Also, the flow rates of the gases are maintained at 100 ml/min. The heating rate of the TGA is set as 10°C/min.

In the thermogravimetric analysis, a DynTHERM (1100-40, MP-G+V) thermogravimetric analyzer (TA Instruments, US) is used. This TGA analyzer is developed based on a magnetic suspension balance (MSB) technology. The MSB technology allows for the measurement of weight changes under vacuum or high pressure. Meanwhile, the gas dosing system of the TGA allows for accurate dosing and blending that are crucial to achieving precise atmosphere control.

TABLE I exhibits the specification of the DynTHERM TGA used in the experimental study.

TABLE I. Specifications of DynTHERM (1100-40, MP-G+V) TGA

MSB		**Temperature**		**Pressure**	**Dosing system**
Resolution (μg)	***Mass range (g)***	***Min (°C)***	***Max (°C)***	***Max (bar)***	
10	25	Room temperature	1100	40	Pure, mixed gases, vapor

Aluminum oxide crucibles with a height of 12 mm and a diameter of 10 mm are used for all the experiments. The morphology of samples before and after experiments are

examined using a field emission scanning electron microscopy (Zeiss Sigma VP FESEM).

B. Case study

This section illustrates the system layout of the TCES system developed in the case study, which is based on the pressurized oxidation of Cu_2O. Also, the simulation flowsheet and key performance indicators of the proposed TCES system are explained.

1) System description

Fig. 2 demonstrates the schematic diagram of the proposed TCES based on the pressurized oxidation of Cu_2O. As can be seen in Fig. 2, the proposed TCES system consists of energy charging and energy discharging processes.

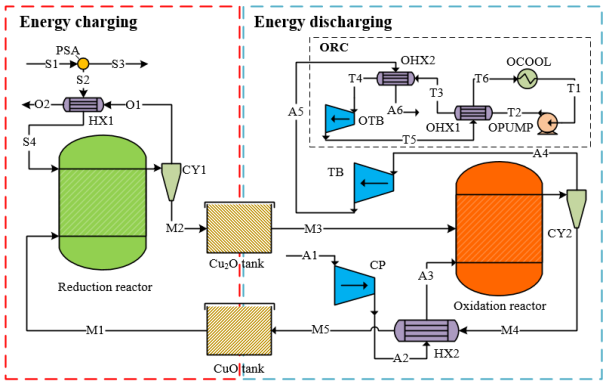

Fig. 2. Schematic diagram of the proposed TCES system

In the energy charging process, CuO particles (M1, see Fig. 2) are initially transported from a CuO tank to a reduction reactor by using a pneumatic conveyor. Meanwhile, ambient air (S1) is introduced into a pressure swing adsorption (PSA) plant that is set to generate N_2-rich sweeping gas (S2). In the reduction reactor, CuO particles are heated to about 950°C and then decomposed to Cu_2O and O_2 with the presence of the sweeping gas. The products with solid and gas are separated in a cyclone (CY1). The separated Cu_2O (M2) is stored in a Cu_2O tank with excellent insulation while the hot gas (O1) passes a gas-gas heat exchanger (HX1) where the waste heat is transferred to the sweeping gas (S2). Hence, the energy input of the reduction reactor is converted to the thermochemical heat stored in the produced Cu_2O.

In the energy discharging process, ambient air (A1) is compressed to around 10 bar in an air compressor. The pressurized air (A2) at a temperature of over 300°C is then preheated in a heat exchanger (HX2). The preheated air (A3) is introduced into an oxidation reactor to oxidize the reduced Cu_2O (M3) coming from the Cu_2O tank. This oxidation takes place at the same pressure as the pressurized air. In this step, the stored heat is recovered and the preheated air (A3) is heated to about 870°C. After oxidation, the hot air is separated from the solid particles in another cyclone (CY2). Then, the hot air (A4) at high pressure expands in an air turbine (TB) to generate power via an air Brayton cycle before being discharged as exhaust air (A5). Meanwhile, the separated solid particles (M4) are introduced to a gas-solid heat exchanger (HX2) where the waste heat is partially transferred to the incoming pressurized air (A2). In order to recover the waste of the exhaust air (A5), a bottoming organic Rankine cycle (ORC) is also employed, as can be seen in Fig. 2.

Fig. 3 shows the equilibrium oxygen partial pressure and temperature under which the reduction or oxidation of CuO/Cu_2O is spontaneous. As can be seen from Fig. 3, low oxygen partial pressure is preferred for spontaneous reduction while high oxygen partial pressure helps achieve oxidation.

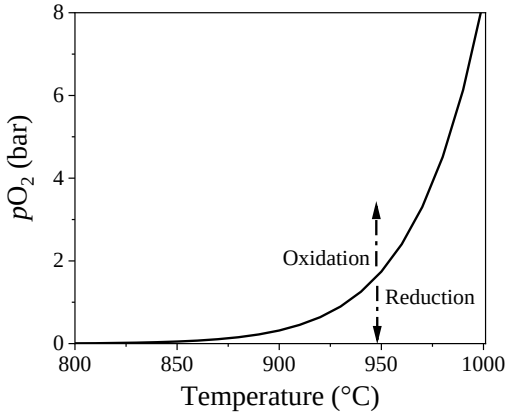

Fig. 3. Equilibrium oxygen partial pressure as a function of temperature in the redox reaction of CuO/Cu_2O

2) Simulation flowsheet

Aspen Plus v10 is employed to model the proposed TCES system based on the pressurized oxidation of Cu_2O in the current research. The solid processing method, property method, and reactor models used in the modeling work can be referred to [21]. The conversion of reduction and oxidation is determined by the equilibrium reaction conditions (i.e., temperature and oxygen partial pressure) in addition to the reactivity of metal oxides. Specifically, the reaction conditions determine whether the specific reaction is spontaneous while the reactivity determines the extent of the reaction. In this study, the equilibrium reaction conditions can be referred to Fig. 3 and the reactivity data are obtained from the TGA tests. Fig. 4 shows the simulation flowsheet of the proposed TCES system in Aspen Plus v10.

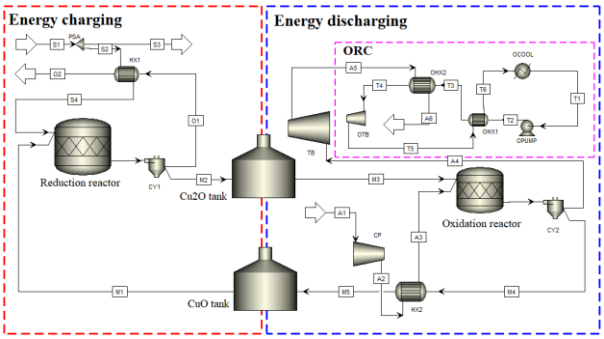

Fig. 4. Simulation flowsheet of the proposed TCES system in Aspen Plus v10

TABLE II shows the main parameters employed in the modeling study. TABLE III displays the specific parameters of the ORC bottoming cycle. It is noteworthy that the simulation parameters of the ORC are adapted from [22].

Round-trip efficiency and energy storage density are calculated to evaluate the energy storage potential of the proposed TCES system.

The round-trip efficiency calculates the amount of electricity that can be recovered for a given energy input:

$$\eta_e = E_{OUTPUT} \times 100\% / E_{INPUT} \quad (1)$$

TABLE II. Main parameters of the modeling study of the proposed TCES system

Component	Parameter	Value
Ambient	Temperature	25°C
	Pressure	1.01 bar
PSA	Energy consumption	$\ln(0.21/0.01)^2$ kJ/mol [23]
	Specified yield	50% [24]
	Mole fraction of N_2	99%
Reduction reactor	Energy input	30 MW
	Temperature	1050°C
	Pressure	1.01bar
Oxidation reactor	Temperature	950°C
	Reactivity of Cu_2O	70%
Compressor (COMP)	Discharge pressure	5.00-15.00 bar
	Isentropic efficiency	89%
	Mechanic efficiency	98%
Turbine (TB)	Discharge pressure	1.01 bar
	Isentropic efficiency	90%
	Mechanic efficiency	98%
Heat exchanger (HX1)	Minimum temperature approach	15°C
Heat exchanger (HX2)	Minimum temperature approach	30°C
Charging/discharging period	-	1 hour

TABLE III. Simulation parameters of the ORC bottoming cycle

Component	Parameter	Value
Heat exchangers (OHX1 and OHX2)	Minimum temperature approach	10°C
ORC turbine (OTB)	Inlet pressure	31.56 bar
	Outlet pressure	0.05 bar
	Isentropic efficiency	87%
	Mechanic efficiency	98%
ORC pump (OPUMP)	Isentropic efficiency	80%
	Mechanic efficiency	98%
	Discharge pressure	32.86 bar
ORC Cooler (OCL)	Outlet temperature	30°C

where η_e represents the round trip efficiency, %; E_{OUTPUT} refers to the power output during the energy discharging process, MWh; E_{INPUT} represents the energy input during the energy charging process, MWh.

E_{OUTPUT} is calculated based on the power output of the air Brayton cycle coupled with the bottoming ORC:

$$E_{OUTPUT} = E_{AIR} + E_{ORC} \quad (2)$$

where E_{AIR} represents the power output of the air Brayton cycle, MWh; E_{ORC} represents the power output of the ORC bottoming cycle, MWh. E_{AIR} and E_{ORC} can be obtained as follows:

$$E_{AIR} = E_{TB} - E_{CP} \quad (3)$$

$$E_{ORC} = E_{OTB} - E_{OPUMP} \quad (4)$$

where E_{TB} represents the power output of the air turbine, MWh; E_{CP} represents the energy demand of the air compressor, MWh; E_{OTB} represents the power output of the ORC turbine, MWh; E_{OPUMP} represents the energy demand of the ORC pump, MWh.

E_{INPUT} can be calculated according to the energy consumed in the reduction reactor and the PSA:

$$E_{INPUT} = E_{REDUC} + E_{PSA} \quad (5)$$

where E_{REDUC} refers to the energy consumed in the reduction reactor, MWh; E_{PSA} refers to the energy consumed in the PSA, MWh.

The energy storage density is defined as the power generated per unit mass of the raw material CuO:

$$\rho_e = E_{OUTPUT} \times 3.6 \times 10^6 / m_{CuO} \quad (6)$$

where ρ_e represents the energy storage density, kJ/kg; m_{CuO} represents the required mass of CuO, kg.

III. Results and Discussions

In this section, the experiment results of the pressurized oxidation are revealed and discussed. Then, the energy storage performance of the proposed TCES system is analyzed according to the case study.

A. Experiment results

The experiment results include the single-cycle TGA tests, multi-cycle TGA tests, and morphology changes of tested samples.

1) Single-cycle test

Fig. 5 shows the single-cycle TGA results of CuO/Cu_2O with a short isothermal period under 1.2 bar, 5.0 bar, and 10.0 bar. The pressure of 1.2 bar is treated as near-ambient pressure considering the pressure drop in the TGA setup. In each specific test, the gas swings from N_2 to air but the pressure is kept the same. The temperature of the sample is gradually heated from room temperature to 950°C and then maintained in a short isothermal period of 10 min before being decreased to 200°C.

According to Fig. 5, all the single-cycle tests show a reduction step and an oxidation step. The start temperature of reduction varies slightly among the three tests due to the different oxygen partial pressures. As the reduction begins, the influence of the oxygen partial pressure becomes more significant. Specifically, the TGA test under 1.2 bar achieves the fastest reduction, which is followed by the TGA test under 5.0 bar. As a comparison, the TGA test under 10.0 bar shows the slowest reduction. Meanwhile, the percentage of weight change in the reduction step accounts for 9%, 4%, and 2% for the TGA tests at 1.2 bar, 5.0 bar, and 10.0 bar, respectively.

This phenomenon can be explained by the equilibrium oxygen partial pressure. As analyzed in Fig. 3, low oxygen partial pressure is beneficial to shift the reaction towards reduction. The oxidation takes place when the flowing gas is changed from N_2 to air, as illustrated in Fig. 5. Compared to the reduction reaction, the oxidation reaction is found to be the same in the three tests. Specifically, the weight percentage recovers to above 99% in about 10 min for all the three tests.

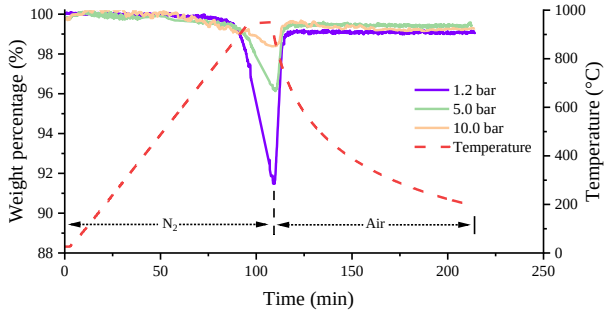

Fig. 5. Single-cycle TGA tests of CuO/Cu_2O with a short isothermal period under different pressures

Fig. 6 shows the single-cycle TGA results of CuO/Cu_2O with a long isothermal period under different oxidation pressures. It is noteworthy that the isothermal period is set as 100 min to ensure complete reactions.

According to Fig. 6 (a), the reduction of CuO does not take place when the temperature reaches 950°C under the air. In contrast, the reduction is found to occur only when N_2 is introduced. The reduction of CuO is accomplished in around 25 min when the weight is decreased by about 10%. On the other hand, when air is introduced to the crucible, the oxidation reaction starts and the weight percentage recovers to around 100% after 10 min. This means that the reduced Cu_2O is fully oxidized back to CuO. Also, it can be concluded that the oxidation is faster than the reduction. Similar oxidation behavior is also found in the oxidation of Cu_2O under 5.0 bar (see Fig. 6 (b)). It is found that the pressurized oxidation under 5.0 bar is completed after only 8 min, which indicates a decrease of 2 min compared to the single-cycle TGA test under 1.2 bar. This phenomenon can be explained by Le Chatelier's principle: as the pressure of oxidation increases, the redox reaction shifts to the direction that decreases the pressure - oxidation.

2) Multi-cycle test

Fig. 7 demonstrates the 20-cycle TGA results of CuO/Cu_2O at 950°C under 1.2 bar. In this test, N_2 and air are introduced for reduction and oxidation, respectively. From Fig. 7, it can be seen that the first 6 cycles, where the weight loss of each cycle reaches about 10% during reduction, present excellent reversibility. Then, the oxidation becomes slower, particularly at the end of oxidation. For instance, the oxidation lasts 58 min in the 20th cycle, which is significantly slower than the single-cycle tests (see Fig. 5 and Fig. 6). According to Fahim et al. [25], the oxidation is constrained by the ash layer of oxidized metal oxide (i.e., CuO in this case). This ash layer is thick enough to develop a diffusion resistance around the particles, which makes the reduced metal oxide (i.e., Cu_2O) not readily available for the oxidation. Besides the slow oxidation, it is also found that the weight loss decreases from 10% to around 7% during reduction after 20 cycles. This means that the reactivity decreases from 100% to 70%. Similar degradation of reactivity is also found in Wong et al.'s study where the authors attributed it to the sintering of metal oxides [12].

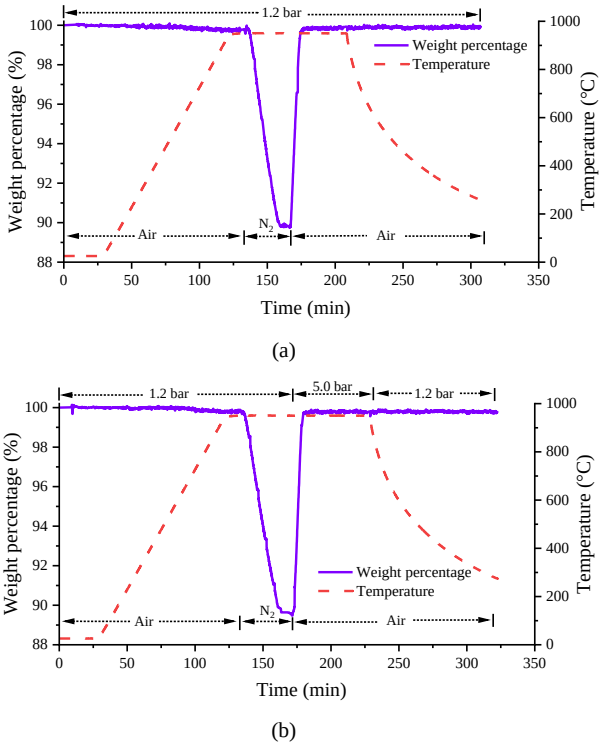

Fig. 6. Single-cycle TGA tests of CuO/Cu_2O with a long isothermal period under different oxidation pressures

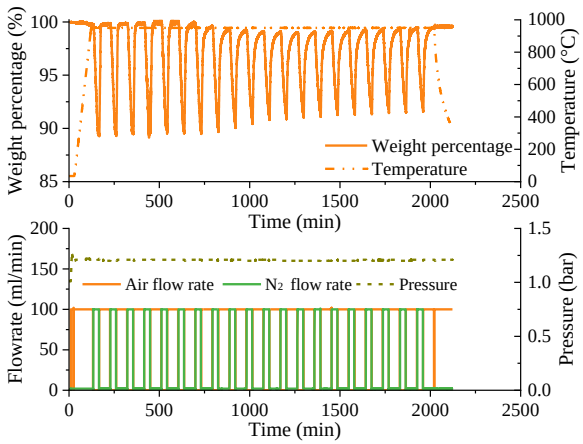

Fig. 7. 20-cycle TGA results of CuO/Cu_2O at 950°C (oxidation pressure of 1.2 bar)

Fig. 8 shows the 20-cycle TGA results of CuO/Cu_2O at 950°C under the oxidation pressure of 5.0 bar. It should be noted that the pressure of reduction is set as 1.2 bar, which is the same as in Fig. 7. As illustrated in Fig. 8, the sample shows improved reversibility compared to the 20-cycle TGA test of CuO/Cu_2O with an oxidation pressure of 1.2 bar. Specifically, the weight loss is found to maintain at around 9% in the performed redox cycles, which indicates a reactivity of 90%. Also, the slow oxidation becomes less significant when the oxidation pressure is elevated to 5.0 bar. Specifically, the oxidation at the end of the 20 cycles is found to last 34 min. Hence, it can be concluded the pressurized oxidation of Cu_2O

under 5.0 bar helps maintain high reversibility and high oxidation rate.

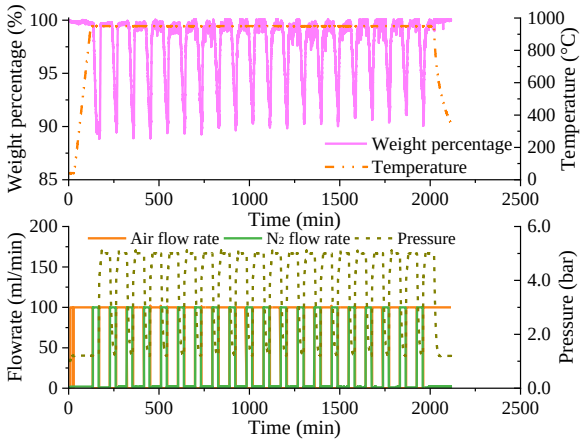

Fig. 8. 20-cycle TGA results of CuO/Cu_2O at 950°C (oxidation pressure of 5.0 bar)

Fig. 9 illustrates the 20-cycle TGA results of CuO/Cu_2O at 950°C under the oxidation pressure of 10.0 bar. As shown in Fig. 9, the first cycle shows a complete redox cycle where the weight loss achieves the theoretical value of 10%. However, the weight loss of the second cycle dramatically drops to 7.5%. A possible explanation is that the time of reduction is not long enough to ensure a complete reduction after the first cycle. Nevertheless, the reactivity keeps relatively stable at around 70% until the 20th redox cycle. Besides, it is found that the oxidation step in the 20th cycle only lasts 20 min.

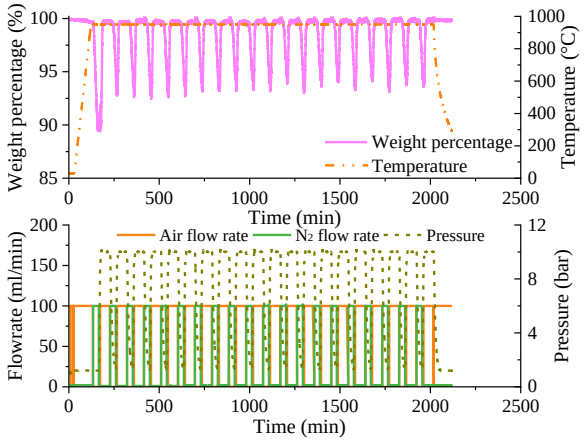

Fig. 9. 20-cycle TGA results of CuO/Cu_2O at 950°C (oxidation pressure of 10.0 bar)

Fig. 10 shows the result of the 20-cycle TGA results of CuO/Cu_2O at 950°C under an oxidation pressure of 15.0 bar. In this case, the reduction time is extended from 30 min to 40 min compared to the 20-cycle TGA test under 10.0 bar (see Fig. 9). According to Fig. 10, the second redox cycle shows a significantly reduced weight loss when compared to the first redox cycle. This phenomenon is similar to the results obtained from the multi-cycle test under 10.0 bar. In Fig. 10, the weight loss fluctuates but still reaches around 8% at the end of the test. This means the reactivity (i.e., 80%) is around 11% higher than the corresponding value in the redox cycles under 1.2 bar. Besides, fast oxidation at the last redox cycle, which completes in 30 min, is also found in this test.

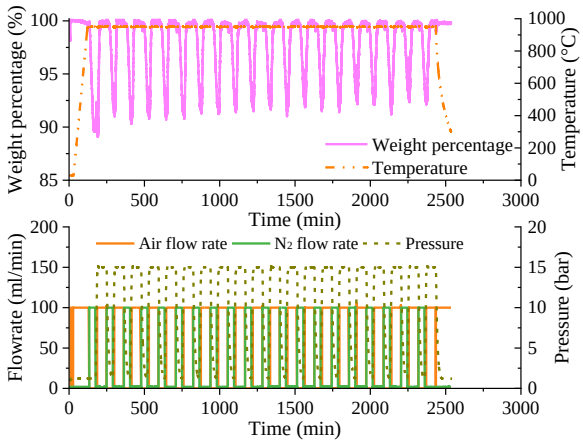

Fig. 10. 20-cycle TGA results of CuO/Cu_2O at 950°C (oxidation pressure of 15.0 bar)

3) Morphology changes

Fig. 11 compares the morphology of CuO/Cu_2O before and after the single-cycle TGA tests. As illustrated in Fig. 11 (a), the fresh CuO sample presents a clear powder form. However, according to Fig. 11 (b-f), the particles begin to agglomerate and sinter after tests. Meanwhile, by comparing Fig. 11 (a-b) and Fig. 11 (c-d), it can be seen that the sintering effect is more significant when the isothermal time is longer. For instance, the samples tested in short isothermal periods are found to remain a powder form although the agglomeration appears (see Fig. 11 (b-d)). By contrast, the particle size of the samples tested in the long isothermal periods is significantly larger (see Fig. 11 (e-f)).

Fig. 12. illustrates the morphology of the samples tested for 20 redox cycles. According to Fig. 12., the sintering effect appears to be more significant over the 20 redox cycles when compared with the single tests. The sintering effect leads to a drop in surface area and eventually results in the loss of the reactivity. Meanwhile, there is no visible difference between the samples tested under different oxygen pressure. To relieve the sintering effect, a possible solution is using different reactors that enhance the heat and mass transfer, such as rotary kiln [16] and fluidized bed [25].

B. Case study

TABLE IV demonstrates the simulation results of the proposed TCES system based on the pressurized oxidation of Cu_2O. From TABLE IV, it can be seen that the reduction reactor consumes around 94% of the total energy input in the energy charging process. By contrast, the energy consumption of the PSA is relatively low, which occupies about 6% of the total energy demand. In the energy discharging process, it is found that more than half of the power output of the air turbine is consumed by the air compressor. This phenomenon is more significant as the oxidation pressure increases. On the other hand, the energy demand of the ORC pump only consumes a small portion of the energy generated by the ORC turbine. Meanwhile, it can also be seen from TABLE IV that the temperature of the exhaust air (A5) decreases gradually as the oxidation pressure increases. The increase of oxidation pressure leads to an increase in the energy output of the air Brayton cycle.

Fig. 13 illustrates the round-trip efficiency and energy storage density of the proposed TCES system under different

oxidation pressures. As can be seen from Fig. 13, the round-trip efficiency increases gradually from 39.0% under the oxidation pressure of 5.0 bar and then peaks at 41.0% under 10.0 bar. However, as the oxidation pressure further increases to 15.0 bar, the round-trip efficiency drops slightly to 40.7%. Hence, it can be concluded that the optimum oxidation pressure for achieving the highest round-trip efficiency is 10.0 bar. On the other hand, Fig. 13 also shows how the energy storage density changes with the oxidation pressure. As the oxidation increases, the energy storage density is found to increase and achieve its highest value of 554.3 kJ/kg under 7.5 bar. Afterward, the increasing oxidation pressure, instead, results in a gradual drop in the energy storage density.

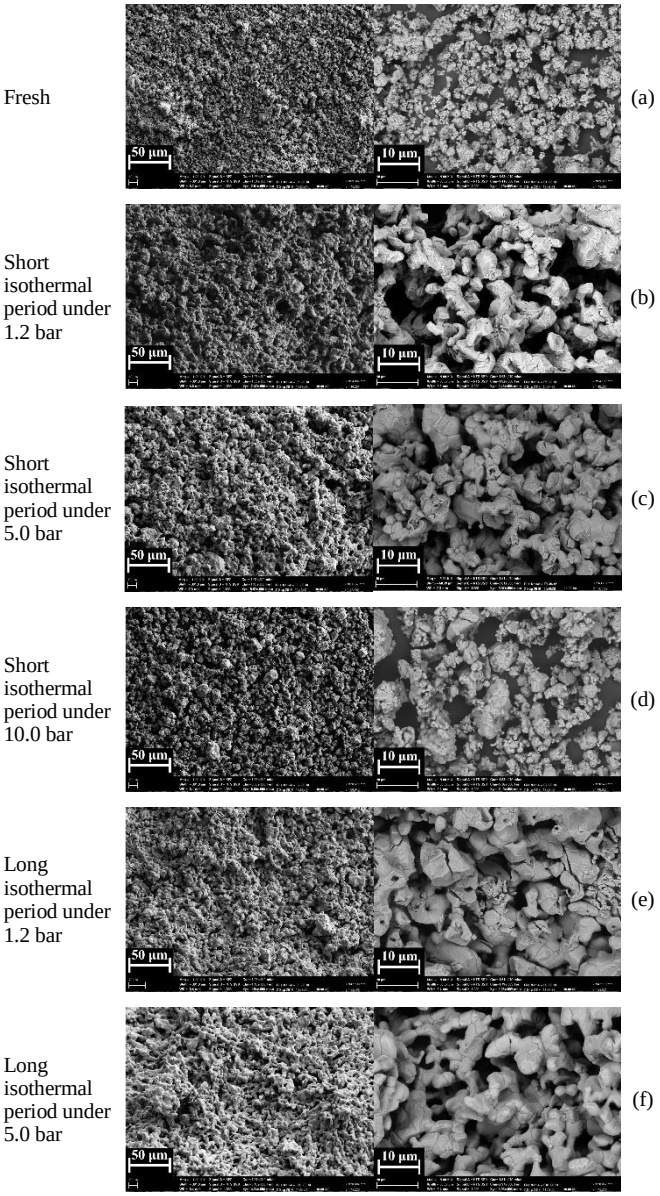

Fig. 11. SEM results of raw material and samples after single-cycle tests

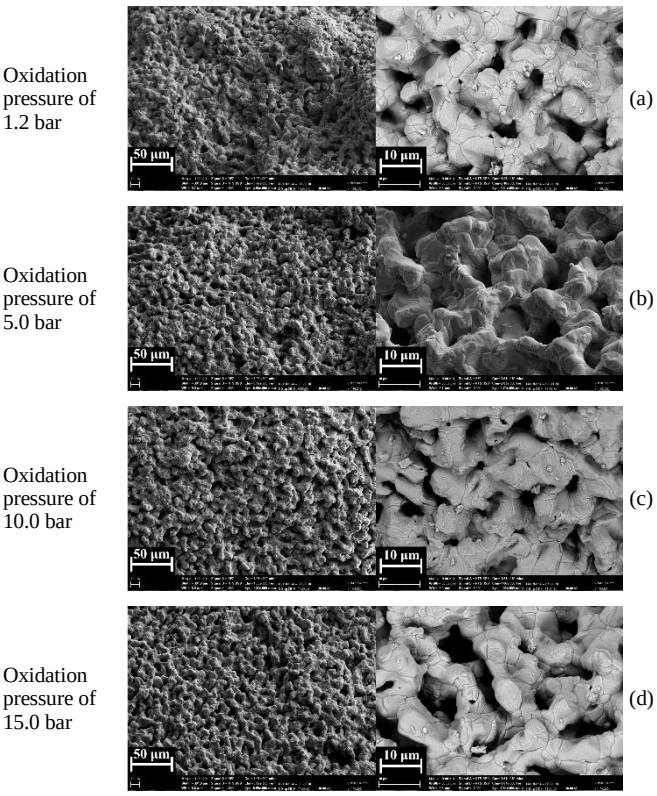

Fig. 12. SEM results of CuO/Cu_2O after 20-cycle TGA tests

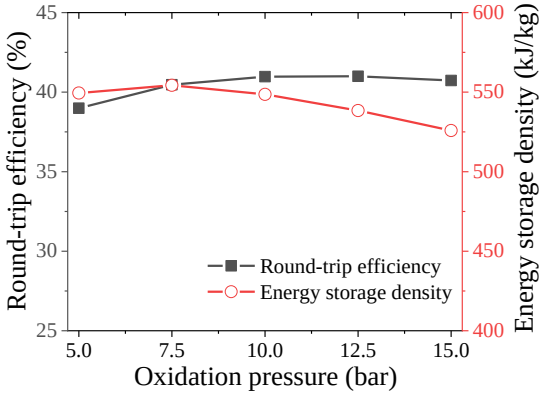

Fig. 13. Round-trip efficiency and energy storage density of the proposed TCES system under different oxidation pressures

TABLE IV. Simulation results of the proposed TCES system under different oxidation pressures

Results	Unit	5.0 bar	7.5 bar	10.0 bar	12.5 bar	15.0 bar
Reduction reactor	MWh	30.00	30.00	30.00	30.00	30.00
PSA	MWh	2.01	2.07	2.12	2.17	2.21
Total energy input	MWh	32.01	32.07	32.12	32.17	32.21
Air turbine	MWh	13.95	18.17	21.60	24.63	27.43
Air compressor	MWh	7.19	10.41	13.35	16.14	18.85
Energy output of air Brayton	MWh	6.77	7.76	8.25	8.49	8.58
ORC turbine	MWh	5.84	5.34	5.03	4.81	4.65
ORC pump	MWh	0.13	0.12	0.11	0.11	0.11
Energy output of ORC	MWh	5.71	5.22	4.91	4.70	4.54
Total energy output	MWh	12.48	12.98	13.16	13.19	13.12
Temperature of exhaust air (A5)	°C	587.28	513.60	465.34	430.08	402.57

TABLE V shows the properties of each stream in the case study under an oxidation pressure of 10.0 bar.

TABLE V. Thermodynamic properties of the streams in the proposed TCES system under an oxidation pressure of 10.0 bar

ID	p (bar)	T (°C)	m (tonne/h)	CuO (mol%)	Cu_2O (mol%)	N_2 (mol%)	O_2 (mol%)	Toluene (mol%)
A1	1.01	25.00	151.25	0.00	0.00	79.00	21.00	0.00
A2	10.00	327.07	151.25	0.00	0.00	79.00	21.00	0.00
A3	10.00	540.14	151.25	0.00	0.00	79.00	21.00	0.00
A4	10.00	950.00	142.57	0.00	0.00	83.31	16.69	0.00
A5	1.01	465.34	142.57	0.00	0.00	83.31	16.69	0.00
A6	1.01	110.70	142.57	0.00	0.00	83.31	16.69	0.00
M1	10.00	357.07	86.37	100.00	0.00	0.00	0.00	0.00
M2	1.01	1050.00	77.68	0.00	100.00	0.00	0.00	0.00
M3	1.01	1050.00	77.68	0.00	100.00	0.00	0.00	0.00
M4	10.00	950.00	86.37	100.00	0.00	0.00	0.00	0.00
M5	10.00	357.07	86.37	100.00	0.00	0.00	0.00	0.00
T1	0.05	25.00	84.76	0.00	0.00	0.00	0.00	100.00
T2	32.86	26.21	84.76	0.00	0.00	0.00	0.00	100.00
T3	32.86	105.70	84.76	0.00	0.00	0.00	0.00	100.00
T4	31.56	300.00	84.76	0.00	0.00	0.00	0.00	100.00
T5	0.05	136.75	84.76	0.00	0.00	0.00	0.00	100.00
T6	0.05	36.21	84.76	0.00	0.00	0.00	0.00	100.00
T7	0.05	25.00	84.76	0.00	0.00	0.00	0.00	100.00
O1	1.01	1050.00	43.89	0.00	0.00	81.39	18.61	0.00
O2	1.01	245.29	43.89	0.00	0.00	81.39	18.61	0.00
S2	1.01	25.00	35.21	0.00	0.00	99.00	1.00	0.00

IV. CONCLUSIONS

In this study, the influence of pressurized oxidation on a pure copper oxides-based thermochemical energy storage system is examined experimentally. Specifically, thermogravimetric analyses and scanning electron microscopy are applied to evaluate the redox behaviors and morphology changes of pure CuO/Cu_2O.

According to the results, the oxidation of Cu_2O, which appears to be the rate-limiting step, is found to be faster under 5.0-15.0 bar compared to the near-ambient condition. For instance, the oxidation steps in the 20th cycle of the tests under 5.0-15.0 bar last around 20-30 min, which is around half of the 58 min found in the redox test under 1.2 bar. Meanwhile, the tests of 20 redox cycles reveal that the reactivity of Cu_2O under 5.0-15.0 bar can maintain 70-90% although the sintering of particles is still present. This finding indicates the excellent reversibility of CuO/Cu_2O under high pressure compared to the test under ambient condition. Based on the thermodynamic analysis in a case study, the proposed TCES plant can achieve a round-trip efficiency of about 41.0% and an energy storage density of nearly 500 kJ/kg under the oxidation pressure of 10.0 bar.

The current research shows that the proposed TCES system based on the pressurized oxidation of Cu_2O has the potential to realize its energy storage function with excellent performance. Hence, this pressurized oxidation of Cu_2O makes the direct integration of TCES and air Brayton cycle becomes possible. Future work will focus on the kinetic analysis of redox reactions under high pressure and the enhancement of reversibility.

CONFLICTS OF INTEREST

The authors declare no competing financial interest.

ACKNOWLEDGMENT

The authors appreciate the funding that they received from The University of Newcastle. The authors thank Dr. Yun Lin for technical assistance and use of facilities at the Electron Microscope and X-Ray Unit (EMX) at The University of Newcastle.

ABBREVIATIONS

MSB	magnetic suspension balance
ORC	organic Rankine cycle
PCR	phase change redox
PSA	pressure swing adsorption
SEM	scanning electron microscopy
TCES	thermochemical energy storage
TGA	thermogravimetric analysis

REFERENCES

[1] IEA. World Energy Outlook 2019. IEA, Paris, 2019.
[2] I. Dincer. Renewable energy and sustainable development: a crucial review. Renewable & Sustainable Energy Reviews. 4 (2011) 157-175.
[3] F. Díaz-González, A. Sumper, O. Gomis-Bellmunt, R. Villafáfila-Robles. A review of energy storage technologies for wind power applications. Renewable & Sustainable Energy Reviews. 16 (2012) 2154-2171.
[4] K. Schmietendorf, J. Peinke, O. Kamps. The impact of turbulent renewable energy production on power grid stability and quality. The European Physical Journal B. 90 (2017) 222.
[5] X. Luo, J. Wang, M. Dooner, J. Clarke. Overview of current development in electrical energy storage technologies and the application potential in power system operation. Applied Energy. 137 (2015) 511-536.
[6] I. Hadjipaschalis, A. Poullikkas, V. Efthimiou. Overview of current and future energy storage technologies for electric power applications. Renewable and sustainable energy reviews. 13 (2009) 1513-1522.
[7] H. Chen, T.N. Cong, W. Yang, C. Tan, Y. Li, Y. Ding. Progress in electrical energy storage system: A critical review. Progress in Natural Science. 19 (2009) 291-312.
[8] J. Kondoh, I. Ishii, H. Yamaguchi, A. Murata, K. Otani, K. Sakuta, et al. Electrical energy storage systems for energy networks. Energy Conversion and Management. 41 (2000) 1863-1874.
[9] T.M.I. Mahlia, T.J. Saktisahdan, A. Jannifar, M.H. Hasan, H.S.C. Matseelar. A review of available methods and development on energy storage; technology update. Renewable & Sustainable Energy Reviews. 33 (2014) 532-545.
[10] S. Wu, Z. Cheng, E. Doroodchi, R. Nellore, B. Moghtaderi. A review on high-temperature thermochemical energy storage based on metal oxides redox cycle. Energy Conversion & Management. 168 (2018) 421-453.
[11] P. Pardo, A. Deydier, Z. Anxionnaz-Minvielle, S. Rouge, M. Cabassud, P. Cognet. A review on high temperature thermochemical heat energy storage. Renewable and Sustainable Energy Reviews. 32 (2014) 591-610.
[12] B. Wong. Thermochemical heat storage for concentrated solar power. General Atomics 2011.
[13] E. Alonso, A. Gallo, C. Pérezrábago, E. Fuentealba. Thermodynamic study of CuO/Cu_2O and Co_3O_4/CoO redox pairs for solar energy thermochemical storage. SolarPACES 2015. AIP Publishing, Cape Town, South Africa, 2016. pp. 1-8.
[14] D. Chadda, J.D. Ford, M.A. Fahim. Chemical energy storage by the reaction cycle CuO/Cu_2O. International Journal of Energy Research. 13 (1989) 63 73.
[15] M. Deutsch, F. Horvath, C. Knoll, D. Lager, C. Gierlmayer, P. Weinberger, et al. High-Temperature Energy Storage: Kinetic Investigations of the CuO/Cu_2O Reaction Cycle. Energy & Fuels. 31 (2017).
[16] E. Alonso, C. Perez-Rabago, J. Licurgo, E. Fuentealba, C.A. Estrada. First experimental studies of solar redox reactions of copper oxides for thermochemical energy storage. Solar Energy. 115 (2015) 297-305.
[17] S. Wu, C. Zhou, E. Doroodchi, B. Moghtaderi. A unique phase change redox cycle using CuO/Cu_2O for utility-scale energy storage. Energy Conversion and Management. 188 (2019) 366-380.
[18] P. Haseli, M. Jafarian, G.J. Nathan. High temperature solar thermochemical process for production of stored energy and oxygen based on CuO/Cu_2O redox reactions. Solar Energy. 153 (2017) 1-10.

[19] M. Silakhori, M. Jafarian, M. Arjomandi, G.J. Nathan. Experimental assessment of copper oxide for liquid chemical looping for thermal energy storage. Journal of Energy Storage. 21 (2019) 216-221.
[20] S. Setoodeh Jahromy, F. Birkelbach, C. Jordan, C. Huber, M. Harasek, A. Werner, et al. Impact of Partial Pressure, Conversion, and Temperature on the Oxidation Reaction Kinetics of Cu_2O to CuO in Thermochemical Energy Storage. Energies. 12 (2019) 508.
[21] S. Wu, C. Zhou, E. Doroodchi, B. Moghtaderi. Techno-economic analysis of an integrated liquid air and thermochemical energy storage system. Energy Conversion and Management. 205 (2020) 112341.
[22] R. Chacartegui, D. Sánchez, J.M. Muñoz, T. Sánchez. Alternative ORC bottoming cycles for combined cycle power plants. Applied Energy. 86 (2009) 2162-2170.
[23] P.T. Krenzke, J.H. Davidson. On the efficiency of solar H_2 and CO production via the thermochemical cerium oxide redox cycle: the option of inert-swept reduction. Energy & Fuels. 29 (2015) 1045-1054.
[24] A.I. Shirley, N.O. Lemcoff. High‐purity Nitrogen by pressure‐swing adsorption. Aiche Journal. 43 (2010) 419-424.
[25] M.A. Fahim, J.D. Ford. Energy storage using the BaO_2·BaO reaction cycle. The Chemical Engineering Journal. 27 (1983) 21-28.